LES of Turbulent Flow of the Non-Newtonian Fluid: The Mean Flow Quantities

Mohamed Abdi, Meryem Ould-Rouiss, Abdelkader Noureddine

LES of Turbulent Flow of the Non-Newtonian Fluid: The Mean Flow Quantities

Mohamed Abdi [1], Meryem Ould-Rouiss [2] Abdelkader Noureddine [1]

[1] Laboratoire de Mécanique Appliquée, Université USTO Mohamed Boudiaf, BP 1505 Oran EL M'Naouar, Oran, Algeria

[2] Laboratoire de Modélisation et Simulation Multi Echelle, MSME, Université Paris-Est, UMR 8208 CNRS, 5 bd Descartes, 77454 Marne-la-Vallée, Paris, France

E-mail : abdi.mohamed1@live.fr

Abstract

The subject matter of this investigation is that of establishing a better understanding of the rheological and hydrodynamic behaviour of a fully developed turbulent flow of the Non-Newtonian fluids through a cylindrical pipe, in additional to ascertaining the accuracy and reliability of the laboratory code present findings, via analysing and discussing the evolution of the main rheological and flow predicted results. Toward this end, a fully developed turbulent flow of a power-law fluid describing by a shear thinning fluid with a flow index of 0.75 in an isothermal axially stationary cylindrical pipe, with domain length of 20R and an adequate grid resolution of 65^3 gridpoints in the axial, radial and circumferential directions, has been performed numerically by means of a Large eddy simulation (LES) approach with an extended Smagorinsky model, at a simulation's Reynolds number of 4000. The main present findings show a good qualitative agreement with the numerical and experimental data, where these findings suggest that the increased shear rate of the shear thinning fluid results in a pronounced enhancement in the mean axial velocity compared to the Newtonian fluid especially in the logarithmic and the core regions. The apparent viscosity of the shear thinning fluid enhances gradually out of the viscous sublayer towards to the pipe core region where the shear thinning fluid becomes more and more viscous, in turn the friction factor exhibits a slightly attenuation.

Keywords: LES; Turbulent flow; Fully developed; Non-Newtonian; Shear thinning fluid; Shear rate.

1. Introduction

The turbulent flow in an axially pipe is of importance in mechanical and engineering fields and is encountered in a variety of engineering applications such as flow in turbo machines, heat exchange, combustion chambers, nuclear reactors. The Newtonian fluid in such flows has not received a lot of attention over the past decades, which has largely focused on hydrodynamic and thermal properties, there is an extensive literature have been performed by many researchers, where they mainly focused on gaining more understanding of the turbulence phenomena, and on

examining the accuracy of different turbulence-closure models to establish the prediction procedures for the turbulent flow in axially stationary pipe, either experimentally or numerically by performing various types of DNS and LES.

In turn, the non-linear fluids, such as polymers, molten plastics, suspensions and slurries, have been widely utilised in many manufacturing and processing industries, where these types of the industrial fluids can be characterised by several rheological models. Extensive research has been focused on this kind of fluids over the last three decades, where the turbulent flow of the power-law fluids in axially pipe have not received a lot of this attention. The first theoretical and experimental studies performed by Metzner and co-workers during the [1955-1959] [1-3], other measurements performed in a pipe flow [4] and in a channel [5]. In their papers; Dodge 1959 [3] performed for the first time a theoretical analysis for turbulent flow of non-Newtonian fluids through smooth pipe, they have developed a semi-theoretical expression for the pressure loss and mean flow rate permitted the prediction of Non-Newtonian turbulent velocity profiles, and a correlation for friction factors versus Reynolds number. Pinho el al.[4] measured the mean axial velocity and of the three normal stresses in fully developed pipe flow with four concentrations of a polymer (sodium carboxymethyl cellulose) shear-thinning solutions and with water, in range of Reynolds numbers from 240 to 111,000. With advance of large scale computers, serval studies have been performed numerically to provide missing details and enhance our knowledge on the turbulence field of non-Newtonian fluids in circular pipe flow, Among them [6-15]. In their papers; Malin [6] presented a fully developed laminar and turbulent flow of power-law fluids in a cylindrical stationary smooth tube are investigated numerically at different Reynolds numbers for and various power law index, he used a modified version of the Lam-Bremhorst K-ε model in turbulent flow, this model is shown to produce good agreement with experiment over a wide range of the generalised Reynolds number and values for the power-law index. Rudman et al [10] performed a fully developed turbulent flows of power-law fluids (shear thinning) in a cylindrical stationary pipe are investigated numerically by the use of DNS at different generalised Reynolds numbers on a domain lengths equals to 4-8πD for various index flow n=0.5, 0.69 and 0.75, they also performed a DNS by using a spectral element-Fourier method. Rudman and Blackburn [11] implemented a spectral element-Fourier method for Direct Numerical Simulation (DNS) of the turbulent flow, the method was applied to the case of turbulent pipe flow in three runs, one for power law the others for Herschel Bulkley fluid at the same generalised Reynolds number Re_g=7500 and the same power law index, with a domain length of 5πD. They applied the same technique to simulate the turbulent flow of blood modelled theologically as a Carreau-Yasuda fluid in a rectangular channel with a streamwise length of 5πD and a spanwise height of 2πD where D is the channel half width at generalised Reynolds number Re_g=3214, they compared their results to the one equation Spalart-Allmaras RANS model. Gnambode et al. [12] performed LES for fully developed turbulent flows of power-law fluids in a cylindrical stationary pipe by using a finite difference scheme, second-order accurate in space and in time, based on a fractional-step method, a dynamic sub-grid-scale model. on a 65^3mesh with length of the domain 20R at different Reynolds numbers Re_s=4000, 8000 and 12000, 8000 and 12000 for various power law index $0.5 \leq n \leq 1.4$. Gavrilov and Rudyak [13] [14] performed DNS fully developed pipe flows of power law fluids, at two generalised Reynolds numbers 10000 and 20000, over the power law index 0.4-1. Gavrilov and Rudyak [13] they focused on turbulent mean quantities by presented the distributions of components of Reynolds stress tensor, averaged viscosity, viscosity fluctuations, and measures of turbulent anisotropy. One year later, [14] reported a same study but this time they focused on the energy balance and the shear stresses by presented the distributions of the turbulent stress tensor components and the shear stress and turbulent kinetic energy balances. More recently, Rudman et

al. [15] examined the effect of the flow index parameter of power-law fluids in turbulent pipe flow are studied by means of direct numerical simulation at a friction Reynolds number 323, to understand the way in which shear thinning or thickening effects on the turbulent kinetic energy production, transport and dissipation in such flows .

It is clear from this literature review, the most relevant numerical research aforementioned previously have been carried out by means of the direct numerical simulation (DNS), there is a lack of data concerning the remaining approaches in such problem. So, that additional numerical data are needed to employ other turbulence models. This study set out to examine the present LES approach with the extended Smagorinsky effectiveness for predicting the turbulent flow of this kind of fluids, to ascertain the accuracy and reliability of the laboratory code predicted results, in additional to discuss the predicted rheological properties, particularly the viscosity and shear rate, as well as the mean flow quantities, especially the mean axial velocity and friction factor of the power-law fluid in the turbulent flow. Toward this end, a large eddy simulation with an extended Smagorinsky model has been applied to investigate numerically a fully developed turbulent pipe flow of a shear thinning fluid with flow index of 0.75 in axially stationary pipe, with an adequate grid resolution of 65^3 gridpoints in in the streamwise, radial and spanwise directions respectively and computational length of 20R at a simulation's Reynolds number of 4000.

2. Governing equations and numerical procedure

2.1 Governing equations

The present study deals numerically with a fully developed of turbulent flow of a shear thinning fluid (n=0.75) fluids in an isothermal axially stationary pipe (Fig.1), by employing a LES approach with an extended Smagorinsky model at a simulation's Reynolds number of 4000. The filtered continuity and filtered momentum equations governing 3D Non-Newtonian fluid are written in a cylindrical coordinate system and are made dimensionless using the centreline axial velocity of the analytical fully developed laminar profile, ($U_{CL}=(3n+1).U_b/(n+1)$) as a reference velocity where U_b is the average velocity, and the pipe radius R as a reference length. The filtered equations can be expressed as follows:

$$\frac{\partial \overline{u}_i}{\partial x_i} = 0 \tag{1}$$

$$\frac{\partial \overline{u}_j}{\partial t} + \frac{\partial \overline{u}_i \overline{u}_j}{\partial x_i} = -\frac{d\overline{P}}{\partial x_j} + \frac{1}{\mathrm{Re}_s}\frac{\partial}{\partial x_i}\left[\overline{\dot{\gamma}^{n-1}}\left(\frac{\partial \overline{u}_j}{\partial x_i} + \frac{\partial \overline{u}_i}{\partial x_j}\right)\right] + \frac{\partial \overline{\tau}_{ij}}{\partial x_i} \tag{2}$$

The overbar symbol ($\overline{\ }$) denotes the filtering operation, $\overline{\tau}_{ij}$ presents the subgrid stress tensor which is associated to the strain rate tensor $\overline{S}_{ij}$ by $\overline{\tau}_{ij} = -2\nu_t \overline{S}_{ij}$, and Re_s is the simulation's Reynolds number which is defined as $Re_s=\rho U_{CL}^{2-n} R^n/K$, where K, n present the consistency and flow index respectively. It is worth nothing that an extended Smagorinsky model has been employed in the current LES runs to closure the eddy viscosity according to [16].

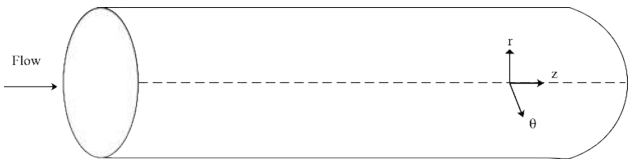

Fig.1 Schematic of the computational domain

2.2 Numerical procedure

The mathematical model was implemented in the laboratory code, the computational procedure is based on finite difference scheme, second-order accurate in space and in time. the time-advancement employs a fractional-step method. a third-order Runge-Kutta explicit scheme and a Crank-Nicholson implicit scheme were used to evaluate the convective and diffusive terms, respectively. The above mathematical model was implemented in a finite difference laboratory code. The governing equations were discretised on a staggered mesh in cylindrical coordinates with an adequate computational length of 20R in the axial direction, where a periodic boundary condition was assigned at the streamwise and spanwise directions, in additional to a No-slip boundary condition applied on the pipe wall. The present computations

are carried out with 65^3 gridpoints in the axial, radial and circumferential directions respectively, the grid mesh in the streamwise and spanwise directions are equally distributed where its dimensionless spaced are of Δz^+=69.89 and $(r\Delta\theta)^+$=21.95 wall unites respectively. A no-equally spaced mesh is applied in the wall normal direction, where the gridpoints are specified by a hyperbolic tangent function with a very small ratio, dimensionless spaced in the radial direction at the wall and pipe centre are of $(\Delta r)_{min}^+$=0.0506 and $(\Delta r)_{max}^+$=12.4 wall unites respectively (Tab.1). It is worth noting that the present LES resolution is better than the moderate resolution: Montreuil [17] showed that LES with Δz^+=35 and $(r\Delta\theta)^+\leq$40 can be considered as LES with high resolution whereas Zang [18] showed that LES with Δz^+<80 and $(r\Delta\theta)^+$<40 can be considered as a moderate resolution.

3. Results and discussion

The present section analyses and discuss critically the main emerged rheological properties, particularly the viscosity and shear rate, as well as the mean flow quantities, especially the mean axial velocity and friction factor of a power-law fluid in the turbulent flow, in order to ascertain the accuracy and reliability of the laboratory code predicted findings, and to examine the large eddy simulation approach effectiveness for predicting the turbulent flow of this kind of fluids, in additional to describe the rheological and hydrodynamic behaviour in such issue. It should be noted that the LES present computational code has already been validated in previous works: for a Newtonian fluid in a rotating pipe at various rotation rates [19][20][21]. Thus, it is confirmed that the present computational LES code is reliable to predict the turbulent velocity and thermal fields for the Newtonian fluid.

3.1 Validation

For the validation purpose, the present LES predictions of the fully developed turbulent flow of a shear thinning fluid (n=0.75) was compared reasonably well with the available results of the literature: the experimental data obtained at generalised Reynolds number of Re_g=7027 and DNS data at Metzner-Reed Reynolds number of Re_{MR}=3935 performed by Rudman et.al [10]. The Fig.2 compares the predicted mean axial velocity profile to those of literature.

Tab.1: parameters of present simulations

Parameter	n=0.75	Parameter	n=0.75
Δz^+	69.89	$\eta_{d,w}$	0.6334
$r\Delta\theta^+$	21.95	Re_{cr}	2250
$\Delta r^+_{\min}$	0.0506	Re_s	4000
$\Delta r^+_{\max}$	12.4	Re_{MR}	4873.2
U_b/U_{cl}	0.5329	Re_g	7135.8
U_c/U_{cl}	0.6863	Re_τ	227.16
U_τ/U_{cl} 10^1	0.3393	Y_1^+	0.0239
$\dot{\gamma}_{d,w}$	6.6818	f $.10^3$	9.2099

Overall, the predicted velocity profile turns out to be in an excellent agreement with the experimental and DNS data over the entire pipe radius, where it is apparent that no significant noteworthy differences were marked between them: the predicted profile almost coincides with these profiles in each of the viscous sublayer $0\leq Y^+\leq 5$, buffer region $5\leq Y^+\leq 30$ and logarithmic layer $30\leq Y^+\leq 200$.

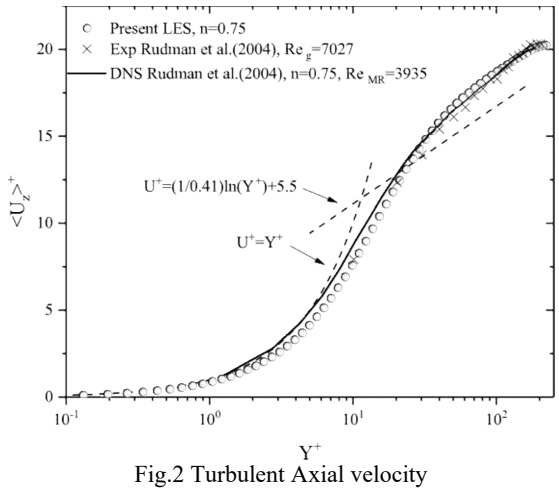

Fig.2 Turbulent Axial velocity

3.2 Mean normalized shear rate and viscosity

The following provides an overview of the shear rate and apparent viscosity of a shear thinning (n=0.75) and Newtonian (n=1) fluids at a simulation's Reynolds number of 4000. The Figure.3 and Figure.4 depict respectively the predicted mean shear rate and apparent viscosity distributions along the pipe radius versus the distance from

the wall in wall units Y^+. As shown in Fig.3, the values of the shear rate of the shear thinning fluid lies sensibly higher than the corresponding values for the Newtonian fluid over the entire pipe radius especially in the vicinity of the wall.

The shear rate of the shear thinning fluid is nearly constant and equals to its peak value in the viscous sublayer, which it can be explained by the viscous force dominant compared to the inertia one in this region ($0 \leq Y^+ \leq 5$). In turn, a marked attenuation of the shear rate profile is observed beyond $Y^+=5$, where the shear rate begins to decrease gradually away from the wall towards the pipe centre with the distance from the wall, which indicates that the inertia force grows progressively with the distance from the wall, which results in a decrease in the viscous one.

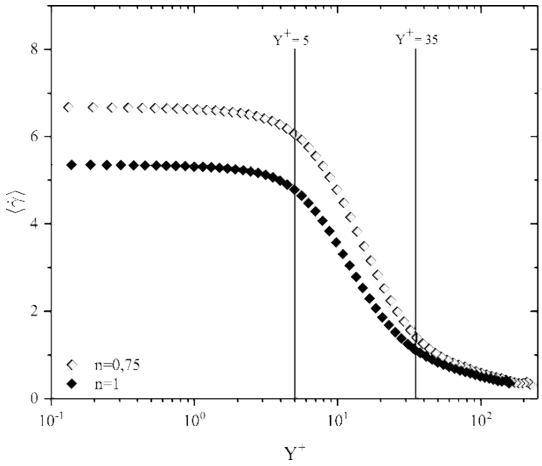

Fig. 3 Behaviour of Mean Dimensionless Shear Rate

Looking at Figure 4, the mean apparent viscosity of the Newtonian fluid is nearly constant along the pipe radius and equals to the wall apparent viscosity; while for the shear thinning fluid (n=0.75) the apparent viscosity is also nearly constant, but just in the vicinity of the pipe wall (viscous sublayer $0 \leq Y^+ \leq 5$). Beyond $Y^+=5$ the fluid's apparent viscosity seems significantly increase with the wall distance increasing, where the fluid's apparent viscosity enhances gradually away from the pipe wall towards the core region with the distance from the wall, the shear thinning fluid (n=0.75) becomes more and more viscous in each of the buffer layer ($5 \leq Y^+ \leq 30$), log layer ($30 \leq Y^+ \leq 200$) and core region ($Y^+ \geq 200$), the fluid tends to behave as a solid when approaching the pipe centre: the pronounced enhancement in the fluid's apparent viscosity is attributed to the shear rate attenuation in these regions.

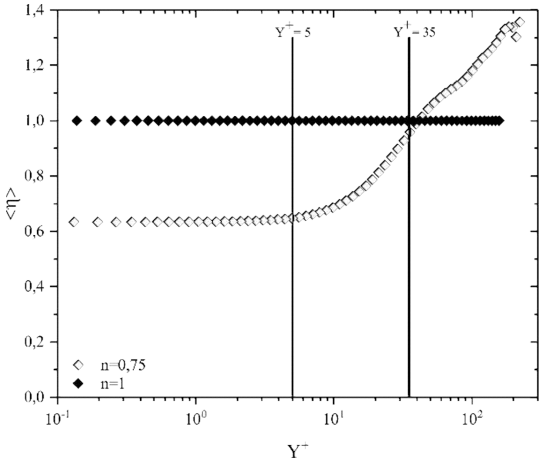

Fig.4 Behaviour of the Dimensionless Mean Viscosity

In order the reveal the association between the fluid's apparent viscosity and the flow's shear rate, the Fig.5 presents the distribution of the apparent viscosity of the shear thing fluid (n=0.75) scaled by the wall viscosity against the shear rate scaled by the wall shear rate. As demonstrate in Fig.5, the apparent viscosity of the Newtonian fluid is constant over the pipe radius and equals to the wall apparent viscosity where is totally independent of the flow's shear rate. As for the shear thing fluid (n=0.75), the shear rate increase results in a significant reduction in the fluid's apparent viscosity over the pipe radius, where the apparent viscosity attenuates monotonically and attains the value of the wall apparent viscosity. The attenuation in the apparent viscosity is attributed to the increase of the shear rate: the mean apparent viscosity is a function of the shear rate and it is inversely proportional to shear rate for the shear thinning fluids (n<1). As shown above, shear rate decrease leads to an enhancement of the fluid's apparent viscosity in each of the buffer layer, logarithmic sublayer and core region as presented in Fig.4, these findings confirm the association between the viscosity and the shear rate where $\eta = K\dot{\gamma}^{n-1}$.

3.3 Mean Velocity Profile

The following paragraphs briefly describe the distribution of the mean streamwise velocity of the shear thinning fluid along the pipe radius in the different turbulent layers. The Fig.6 set out the shear thinning (n=0.75) and Newtonian fluids mean axial velocity distributions scaled by friction velocity $U_\tau = \sqrt{\tau_w / \rho}$ along the pipe radius, versus the distance from the wall in wall units Y^+ , the dash lines represent the universal velocity distributions in the viscous sublayer($0 \le Y^+ \le 5$) and the logarithmic layer ($30 \le Y^+ \le 200$).

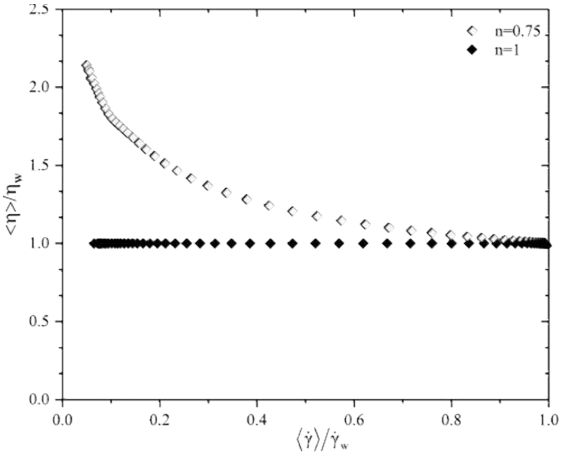

Fig.5 Mean Apparent Viscosity

As shown in Fig.6, the Newtonian profile resolves the universal linear law $U^+=Y^+$ and the universal logarithmic law $U^+=2.5\ lnY^+ +5.5$. As for the shear thinning fluid (n=0.75), the profile coincides totally with the Newtonian one in the vicinity of the wall, the predicted axial velocity remains constant and obeys the universal linear law $U^+=Y^+$, denoting a linear velocity distribution in the viscous sublayer ($0 \le Y^+ \le 5$). At the larger distances from the wall, the predicted velocity exhibits a minor deviation from the Newtonian profile, this trend is more pronounced as the distance from the wall Y^+ is increased in the logarithmic layer ($30 \le Y^+ \le 200$), where the profile of the shear thinning fluid lies above the Newtonian one: this discrepancy is due to the difference in the fluid's shear rate over this region (Fig.3): the shear rate of shear thinning fluid is higher than the Newtonian one along the pipe radius out of the viscous sublayer ($Y^+ > 5$), the fluid's shear rate enhancement induces a noticeable increase in the fluid layers movement past each other away from the wall with the wall distance (Fig.3) thereby enhancing the mean axial velocity along the pipe radius especially in the logarithmic layer and core region (Fig.4).

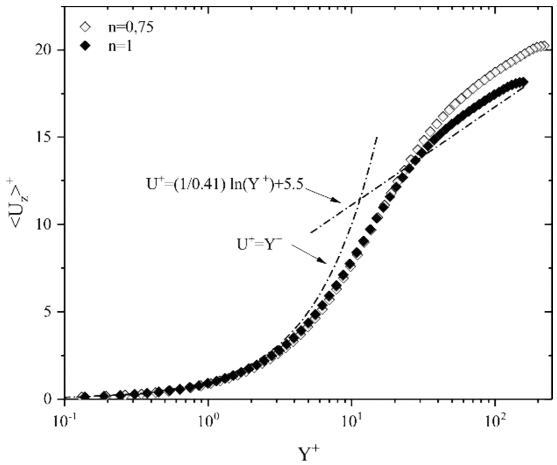

Fig.6 Turbulent Axial Velocity

The figure.7 illustrates the axial mean velocity distribution of the shear thinning fluid (n=0.75) over the pipe radius scales by the analytical laminar centreline velocity ($U_{CL}=(3n+1)U_b/(n+1)$) versus the distance from the wall (Y) scaled by the pipe radius (R), whereas the dash line represents the analytical velocity distribution in the laminar flow. Looking at Fig.7, it is evident that the predicted velocity profile of the shear thinning (n=0.75) has a similar shape to the laminar profile, where these profiles are characterised by a parabolic shape, the velocity profile in the laminar flow are pronouncedly higher than the others in the turbulent flow. As mentioned above, the discrepancy between the profiles of the power-law and Newtonian fluids arises because the difference in the shear rate and viscosity of the fluid.

A snapshot of the instantaneous streamwise velocity field over the cross and longitudinal sections of a shear thinning fluid (n=0.75) is visualised in Fig.8, As clearly observed that the flow vortical structures are propagated along the streamwise and normal wall directions, where the small-scale structures of the flow turbulence are located away from the centerline pipe, the instantaneous turbulence velocity

structure near the pipe wall are small and fine than those in the core region.

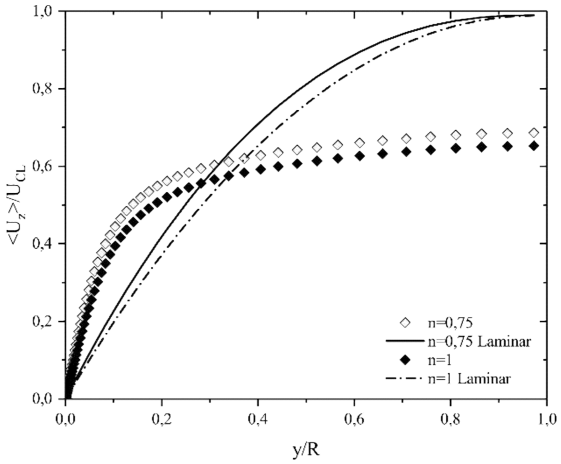

Fig.7 Axial Mean velocity distribution

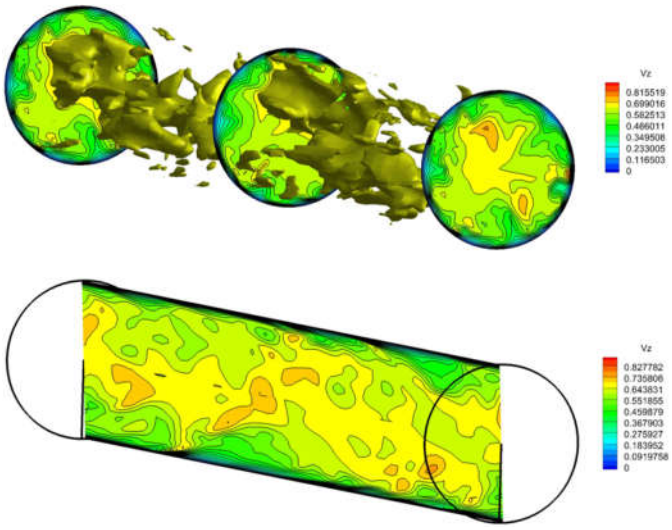

Fig.8 Instantaneous Mean Axial Velocity

It is evident that the friction factor of the shear thinning fluid (n=0.75) attenuates markedly compared to that of the Newtonian fluid: the apparent viscosity of the shear thinning fluid (n=0.75) is lower than that of the Newtonian fluid at the pipe wall (Fig.4), this discrepancy leads to a diminution of the shear thinning fluid friction factor.

Conclusion

A large eddy simulation with an extended Smagorinsky model have been utilised to reported numerically the fully developed turbulent flow of a Non-Newtonian fluid in an axially stationary pipe, where the current modelled fluid was described by a power-law fluid (shear thinning) with flow index of 0.75 at a simulation's Reynolds number of 4000. Many statistical quantities such as; the mean axial velocity profile, the instantaneous mean axial velocity and the friction factor were predicted and compared reasonably with those available in the literature. The current investigation contributes to our understanding of the rheology and hydrodynamic behaviour of this kind of fluid in the turbulent flow.

The accuracy and reliability of the laboratory code predicted results have been Scrutinised by comparing the present prediction results with those results available in the literature. The main findings suggest that the shear rate of the shear thinning fluid (n=0.75) is more important than that of the Newtonian one out of the viscous sublayer, which it leads to deviate the mean axial velocity of the shear thinning fluid from the Newtonian profile especially in the logarithmic and core region of the pipe flow. Moreover, the fluid's apparent viscosity enhances gradually away from the viscous sublayer towards to the pipe core region where the shear thinning fluid becomes more and more viscous, the fluid tends to behave as a solid when approaching the pipe centre. In additional to the friction factor exhibits a slightly attenuation compared to the Newtonian one.

The study contributes to our understanding of the Non-Newtonian fluid behaviour, where the key strength of the present study was the employ the Large eddy simulation for Non-Newtonian fluid, the findings clearly indicate that the effectiveness of LES to deal with this kind of fluid. Further research could also be conducted to determine the influence of fluid index of the shear thinning fluids.

References

[1] Metzner AB, Reed JC 1955 Flow of non-newtonian fluids-correlation of the laminar, transition, and turbulent-flow regions. AIChE J. 1, 434–440.

[2] Metzner AB 1957 Non-Newtonian Fluid Flow. Relationships between Recent Pressure-Drop Correlations.

Ind. Eng. Chem. 49, 1429–1432.

[3] Dodge DW, Metzner AB 1959 Turbulent flow of non-newtonian systems. AIChE J. 5, 189–204.

[4] Pinho FT, Whitelaw JH 1990 Flow of non-newtonian fluids in a pipe. J. Nonnewton. Fluid Mech. 34, 129–144.

[5] Willmarth WW, Wei T, Lee CO 1987 Laser anemometer measurements of Reynolds stress in a turbulent channel flow with drag reducing polymer additives. Phys. Fluids 30, 933.

[6] Malin MR 1997 Turbulent pipe flow of power-law fluids. Int. Commun. Heat Mass Transf. 24, 977–988.

[7] Malin M. 1997 the Turbulent Flow of Bingham Plastic Fluids in Smooth Circular Tubes. Int. Commun. Heat Mass Transf. 24, 793–804.

[8] Malin M. 1998 Turbulent pipe flow of Herschel-Bulkley fluids. Int. Commun. Heat Mass Transf. 25, 321–330.

[9] Rudman M, Blackburn HM 1999 Large eddy simulation of turbulent pipe flow. In Second International Conference on CFD in the Minerals and Process Industries, Melbourne, Australia, Dec, pp. 6–8.

[10] Rudman M, Blackburn HM, Graham LJW, Pullum L 2004 Turbulent pipe flow of shear-thinning fluids. J. Nonnewton. Fluid Mech. 118, 33–48.

[11] Rudman M, Blackburn HM 2006 Direct numerical simulation of turbulent non-Newtonian flow using a spectral element method. Appl. Math. Model. 30, 1229–1248.

[12] Gnambode PS, Orlandi P, Ould-Rouiss M, Nicolas X 2015 Large-Eddy simulation of turbulent pipe flow of power-law fluids. Int. J. Heat Fluid Flow 54, 196–210.

[13] Gavrilov AA, Rudyak VY 2016 Direct numerical simulation of the turbulent flows of power-law fluids in a circular pipe. Thermophys. Aeromechanics 23, 473–486.

[14] Gavrilov AA, Rudyak VY 2017 Direct numerical simulation of the turbulent energy balance and the shear stresses in power-law fluid flows in pipes. Fluid Dyn. 52, 363–374.

[15] Singh J, Rudman M, Blackburn HM 2017 The influence of shear-dependent rheology on turbulent pipe flow. J. Fluid Mech. 822, 848–879.

[16] Ohta T, Miyashita M 2014 DNS and LES with an extended Smagorinsky model for wall turbulence in non-Newtonian viscous fluids. J. Nonnewton. Fluid Mech. 206, 29–39.

[17] Montreuil E 2000 Simulation numérique pour l'aérothermique avec des modèles sous-maille.

[18] Zang TA 1991 Numerical Simulation of the Dynamics of Turbulent Boundary Layers: Perspectives of a Transition Simulator. Philos. Trans. R. Soc. A Math. Phys. Eng. Sci. 336, 95–102.

[19] Ould-Rouiss M, Dries A, Mazouz A 2010 Numerical predictions of turbulent heat transfer for air flow in rotating pipe. Int. J. Heat Fluid Flow 31, 507–517.

[20] Bousbai M, Ould-Rouiss M, Mazouz A, Mataoui A 2013 Turbulent heat transfer characteristics of water flow in a rotating pipe. Heat Mass Transf. und Stoffuebertragung 49, 469–484.

[21] Ould-Rouiss M, Bousbai M, Mazouz A 2013 Large eddy simulation of turbulent heat transfer in pipe flows with respect to Reynolds and Prandtl number effects. Acta Mech. 224, 1133–1155.